Research on Engineering Structures & Materials
www.jresm.org
MIM Research Group

Research Article

Experimental investigation of UHPC–grout and NC–grout interface bond performance under specified surface treatments

Jing Chen [*,a]

Department of Architectural Engineering and Art Design, Liuzhou City Vocational College, Liuzhou 545036, China

Article Info

Article History:

Received 26 Jun 2026

Accepted 24 Sep 2026

Keywords:

UHPC;
Interface mechanical properties;
Interface treatment;
Shear strength;
Splitting tensile strength;
Offshore wind power

Abstract

In jacket-based strengthening systems, a grout layer can connect a precast ultra-high-performance concrete (UHPC) shell and an existing normal-concrete (NC) substrate, thereby forming two independent interfaces: a UHPC–grout interface and an NC–grout interface. This laboratory study evaluated the splitting-tensile and push-out responses of an untreated UHPC–grout interface and a chiseled NC–grout interface. The experimental design changes substrate type and surface treatment simultaneously; it therefore does not isolate the independent effect of chiseling. For the splitting-tensile test, the means (95% confidence interval, CI) were 3.45 ± 0.02 MPa (3.40–3.50 MPa) for SPN-Z and 3.54 ± 0.12 MPa (3.25–3.82 MPa) for SPU-G (n = 3 per group). The reported two-sided Welch test gave p = 0.324; this result does not establish equivalence. For double-face push-out testing, the complete raw PUN-Z dataset, including PUN-Z-1, gave 3.33 ± 0.38 MPa (n = 3; 95% CI: 2.40–4.27 MPa), while the untreated UHPC–grout dataset gave 1.12 ± 0.12 MPa (n = 2; 95% CI: 0.03–2.20 MPa). The push-out comparison is descriptive and exploratory only: n = 2 is insufficient for general inference, and substrate type and treatment were changed together. Under the present short-term static laboratory conditions, the specimens showed different observed failure appearances. These observations do not establish long-term, marine, durability, or cyclic-loading performance.

© 2026 MIM Research Group. All rights reserved.

1. Introduction

Offshore wind-turbine concrete towers provide the engineering context that motivated this study. However, the present program did not simulate seawater exposure, cyclic loading, or other marine environmental actions. Accordingly, this paper addresses only the short-term static bond response of laboratory-prepared composite specimens and does not make durability or long-term offshore-performance claims. A practical jacket-strengthening configuration may consist of a precast UHPC shell, an intermediate grout layer, and an existing NC substrate. The load-transfer path therefore contains two separate material interfaces, namely the UHPC–grout interface and the NC–grout interface; UHPC and NC do not directly contact each other in the tested configuration. The integrity of both interfaces governs the composite action of the three-layer system [1]. Interfacial bond can be influenced by surface topography, substrate condition, curing, material strength, and the test configuration. Previous studies of directly cast UHPC–NC interfaces indicate that surface roughness and substrate properties can materially affect bond strength and failure mode [2-7]. These findings are used here only as background because the present specimens contain an intermediate grout layer.

*Corresponding author: jchenlcvc@outlook.com
[a]orcid.org/0009-0008-1499-9114
DOI: http://dx.doi.org/10.17515/resm2026-1793im0626rs

The elastic modulus of UHPC is generally higher than that of NC. Published values for UHPC commonly fall in the range of approximately 40–55 GPa, whereas values of 20–30 GPa are typical for many normal concretes; for example, Graybeal [8] reported an elastic modulus of 52.4 GPa for a commercially available UHPC. This stiffness mismatch may produce deformation incompatibility and local stress concentration under load. The measured elastic moduli of the UHPC, NC, and grout used in this study are reported in Section 2.1. Prior work has evaluated direct UHPC–NC interfaces using tensile, shear, and microstructural methods [9-12]. In contrast, systematic data for the two-interface UHPC–grout/NC–grout configuration are limited. Moreover, the present study used a nominal chiseling depth of 3–5 mm without an instrumental roughness measurement; it therefore cannot quantitatively relate bond performance to a roughness parameter. Any mechanism involving hydration products or chemical adhesion is treated below as a hypothesis, not as a directly verified result.

The literature also shows that measured interface properties depend on the selected test configuration and loading boundary conditions. Direct-shear and push-out tests require particular attention to eccentricity, support geometry, and the effective shear area. Double-face specimens are therefore adopted as the main basis for the present shear-strength analysis; single-face results are retained only as reference observations [13-15]. Accordingly, this study has four objectives: (1) to document the splitting-tensile and push-out behavior of UHPC–grout and NC–grout interfaces prepared under the stated conditions; (2) to compare the observed failure modes and load–slip responses; (3) to report the exploratory observed differences between the two confounded experimental groups without claiming an independent surface-treatment effect; and (4) to identify the experimental information required for a rigorous subsequent factorial study. The results are interpreted only under the present experimental conditions. It should be noted that the experimental design does not isolate the effects of substrate type and surface treatment, because chiseled NC–grout interfaces are compared with untreated UHPC–grout interfaces. Therefore, any observed group difference cannot be uniquely attributed to chiseling alone. Future work should include both chiseled-UHPC and untreated-NC groups, with matched specimen geometry and replicated testing.

2. Experimental Materials and Methodology

2.1 Materials Used in the Study

2.1.1 UHPC

The UHPC matrix was prepared from UHPC-120 dry premix (Shanghai Fang Sheng New Material Technology Co., Ltd.), copper-coated micro-steel fibers, and 210 kg/m^3 water. The steel-fiber volume fraction was 2%. The 28-day compressive strengths of three UHPC specimens were 122.3, 127.1, and 124.8 MPa, giving 124.73 ± 2.40 MPa (mean ± sample SD). The corresponding elastic moduli were 47.0, 45.9, and 44.5 GPa, giving 45.80 ± 1.25 GPa. The measured density was 2430 kg/m^3. The UHPC tests were conducted in accordance with T/CECS 864-2021, Standard for Test Methods of Ultra-High-Performance Concrete.

Table 1. UHPC mix design (kg/m^3)

UHPC-120 dry premix (kg/m^3)	Steel fiber (kg/m^3)	Water (kg/m^3)
2100	157	210

Table 2. Physical parameters of steel fibers

Shape Type	Length/	Equivalent	Tensile	Density, ρ (kg/m^3)
Circular-straight	13	0.2	1000	7850

2.1.2 Normal Concrete (NC)

The NC substrate was designated C50. It was produced using P.O. 42.5 Portland cement, medium sand, 5–25 mm crushed aggregate, tap water, and PC-6220 polycarboxylate-ether powder superplasticizer. The full batch quantities, aggregate gradation, sand rate, admixture dosage,

mixing sequence, and available fresh- and hardened-property verification data are reported in Tables 3 and 3a. The 28-day compressive strengths were 63.7, 62.3, and 65.8 MPa, giving 63.93 ± 1.76 MPa; the corresponding elastic moduli were 32.6, 35.4, and 33.8 GPa, giving 33.93 ± 1.40 GPa.

Table 3. Normal concrete mix design (kg/m^3)

Parameter	Reported value	Verification / Note
Cement	P.O. 42.5 Portland cement; 750 kg/m^3	Batch quantity
Crushed aggregate	970 kg/m^3; 5–25 mm	Batch quantity and nominal grading
Fine aggregate	Medium sand, 450 kg/m^3; 0.3–0.6 mm	Batch quantity and nominal grading
Sand rate	31.7%	Fine aggregate as reported for the aggregate fraction
Water	210 kg/m^3	Nominal water-to-cement ratio = 0.28
Admixture	PC-6220 polycarboxylate-ether powder superplasticizer	Water-reducing rate ≥ 25%
Mixing sequence	Dry mix cement, sand, and crushed aggregate; add water last; total mixer running time 4 min	Production procedure
Molding	NC placed in 2–3 layers	Separate vibration/compaction record not available
Slump	140 ± 30 mm	Available fresh-property verification
28-day compressive strength	63.93 ± 1.76 MPa (n = 3)	Values: 63.7, 62.3, and 65.8 MPa

2.1.3 Filler

The intermediate material was the proprietary underwater cementitious grout FS-UW60, supplied by Shanghai Fang Sheng New Material Technology Co., Ltd. The manufacturer does not authorize disclosure of the complete formulation. Within the manufacturer-authorized scope, the available product identity and technical parameters are reported here: the reported initial flow was 293 mm, and the reported 1 d, 7 d, and 28 d compressive strengths were 28.4, 56.9, and 70.3 MPa, respectively. The measured water-to-powder ratio was 0.13; wet density was 2352 kg/m^3; and the initial and final setting times were 175 and 310 min, respectively. The measured 28-day flexural strengths were 12.7, 12.5, and 13.4 MPa, giving 12.87 ± 0.47 MPa, and were determined according to GB/T 17671-2021. The measured 28-day elastic moduli were 34.3, 34.6, and 35.7 GPa, giving 34.87 ± 0.74 GPa (mean ± sample SD). The reported 28-day vertical expansion ratio was 0.04%, which is reported as a dimensional-change indicator rather than as shrinkage. The grout properties were determined using the stated test methods. GB/T 50448-2015 was the applicable technical reference for this cementitious-grout product.

2.2 Specimen Preparation

2.2.1 Manufacturing Procedure for UHPC and NC Composites

- Prepare molds: Prepare corresponding test molds according to the designed dimensions;
- Weigh materials: Batch weigh the materials based on the raw material ratio and the initial mixing capacity, as shown in Fig.1. (a).
- Mix: For NC, the cement, medium sand, and crushed aggregate were dry mixed first; water containing the PC-6220 superplasticizer was added last, and the total mixer running time was 4 min. For UHPC, the weighed dry powder and water were pre-mixed at high speed for 3 min, after which the weighed steel fibers were added in 2–3 portions while continuing low-speed mixing to limit fiber clumping and promote uniform distribution, as shown in Fig.1. (b).

- Pour: To ensure the concrete is formed and compact, NC was filled into the molds in 2 to 3 layers. UHPC mixture was poured into the molds, and the molds were gently vibrated laterally to eliminate entrapped air bubbles.

The UHPC and NC substrate specimens were demolded 24 h after casting. The specimens were covered with plastic film and periodically wetted until the specified 28-day substrate age. The curing temperature, relative humidity, watering frequency, and fresh NC density were not retained in the available batch records and are therefore not reported. In this paper, "28-day substrate age" refers to the age of the UHPC or NC substrate before grout placement.

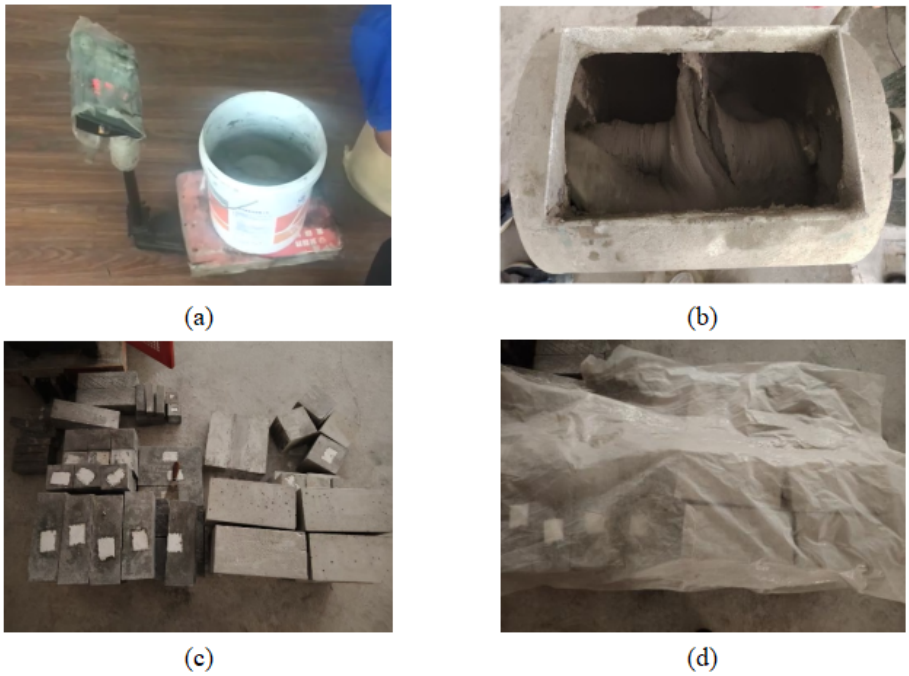


Fig. 1. (a) Material weighing, (b) mixing, (c) demoulding, (d) curing of UHPC and NC substrates

2.2.2 Preparation of Specimens for Interfacial Mechanical Tests

The present programmed examined two independent bonded systems: UHPC–grout and NC–grout. All composite specimens were produced by two-stage casting. The first-stage substrate and the second-stage grout were identified separately in the specimen code and in all subsequent figures and tables.

The double-face push-out specimen shown in Fig. 2(a) had a nominal height of 300 mm and two nominal interface planes of 300 mm × 100 mm. The total bonded area used for the double-face calculation was therefore $A = 2 \times 300 \times 100 = 60000$ mm^2. The splitting-tensile specimen shown in Fig. 2(b) was a 150 mm cube composed of two 75 mm halves.

After substrate casting, the bonding surfaces assigned to the NC–grout group were chiseled to a nominal depth of 3–5 mm, cleaned with water, and returned to the molds. The UHPC–grout group was tested with an untreated surface. Because roughness was not quantified by sand-patch, profilometry, or three-dimensional imaging, "3–5 mm" is a construction description rather than a measured roughness parameter. This limitation is considered in Section 3.3.

The grout was cast after the substrate reached an age of 28 days. Before casting, each bonding surface was moistened to a saturated-surface-dry condition without standing water. At testing, the grout age was seven days; substrate age and grout age are reported separately throughout this paper.

The production and test sequence was as follows: Day 0—cast the UHPC or NC substrate; Day 1 (24 h)—demold the substrate; Day 28—complete substrate curing, apply the surface treatment, clean, and condition the surface; Day 29—cast the grout; Day 30—demold the composite; Day 30–37—cure the grout composite; and Day 37 (grout age 7 d)—test the composite specimen.

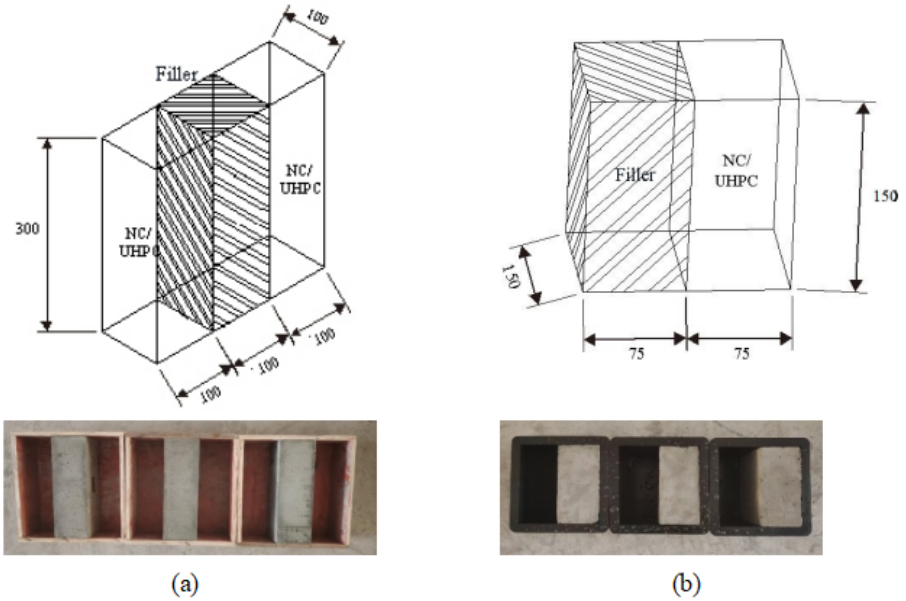


Fig. 2. Specimen geometries and preparation: (a) double-face push-out specimen for UHPC–grout and NC–grout interfaces; (b) 150 mm cubic splitting-tensile specimen. Dimensions are in millimetres

2.3 Experimental Design

Specimen identification follows "test type – substrate – surface treatment – number of shear planes (push-out only) – replicate number". "PU" denotes push-out, "SP" denotes splitting tensile, "U" denotes UHPC, "N" denotes NC, "G" denotes untreated, and "Z" denotes chiseled. Thus, PUU-G-2-1 denotes the first double-face push-out specimen with an untreated UHPC–grout interface, while SPN-Z-2 denotes the second splitting-tensile specimen with a chiseled NC–grout interface. The double-face untreated UHPC–grout dataset comprises PUU-G-2-1 and PUU-G-2-2 only. This nomenclature is used consistently throughout the text, figures, and tables. PUU-G-2-3 was prepared as a strength-check specimen for the double-face UHPC-grout configuration. It is not included in the primary PUU-G push-out dataset, which comprises PUU-G-2-1 and PUU-G-2-2 only.

Table 4. Specimen types for testing

Specimen ID	Substrate–grout interface	Interface processing method	Test Type	Number of specimens
PUU-G-1-	UHPC–grout	Untreated (G)	Single-face push-	3
PUU-G-2-1/2	UHPC–grout	Untreated (G)	Double-face	2
PUN-Z-2-	NC–grout	Chiseled (Z)	Double-face	3
SPU-G-1/2/3	UHPC–grout	Untreated (G)	Splitting tensile	3
SPN-Z-1/2/3	NC–grout	Chiseled (Z)	Splitting tensile	3

2.4 Test Methods

2.4.1 Interfacial Splitting Tensile Test

Splitting-tensile tests were performed on 150 mm cubic composite specimens. The cube was selected because it accommodated two equal 75 mm substrate/grout halves and a planar bonded interface with a defined 150 mm × 150 mm projected area. The loading concept of ASTM C496/C496M-17, which was originally developed for homogeneous cylindrical concrete specimens, was adapted to this bonded cubic configuration, consistent with prior interface studies [9]. This procedure examines splitting across the bonded plane; it is not presented as an unmodified ASTM C496 material-strength test. The testing machine was a 2000 kN electro-hydraulic system (YAW-2000), the loading rate was 1.0 kN/s, and the steel loading strip measured 150 mm × 20 mm

× 3 mm. For a 150 mm cubic specimen, the splitting tensile strength was calculated according to the cubic-splitting formulation of GB/T 50081-2019:

$$f_{ts} = \frac{2P}{\pi A} \tag{1}$$

where f_{ts} is the interfacial splitting-tensile strength (MPa), P is the peak load (N), and A is the projected area of the bonded plane. For every specimen, A = 150 × 150 = 22500 mm^2.

The two 150 mm × 20 mm steel strips were placed on opposing cube faces. Their loading line was centered on and aligned with the bonded plane so that the induced splitting action was directed across the interface. Before loading, the contact faces and bearing plates were ground and cleaned to minimize unintended eccentricity. Each specimen was loaded continuously to failure at 1.0 kN/s. Peak load, crack initiation, and final failure mode were recorded. The fracture path was classified as interfacial (Types A and C) or mixed (Type B); no specimen in Table 6 was classified as a failure occurring wholly within the grout or wholly within the substrate.

2.4.2 Push-Out Test for UHPC/NC-Filler Interface

Push-out tests evaluated the shear response of the UHPC–grout and NC–grout interfaces. The principal strength analysis used only double-face specimens with a total bonded area of 60000 mm^2. Single-face specimens with a 30000 mm^2 bonded area are reported only as reference observations and are not combined with double-face results. The top loading steel plate and the two bottom support steel plates each measured 100 mm × 300 mm × 20 mm. The two lower support plates carried F/2 each and had a center-to-center spacing of 200 mm. Four LVDTs with a resolution of 0.001 mm were arranged symmetrically on the front and rear faces of each specimen; the measurement points were located no more than 50 mm from the shear interface. Load and relative-slip data were acquired at a sampling frequency of 10 Hz, which was increased to 20 Hz when failure approached. The loading protocol consisted of monotonic force-controlled loading at a constant rate of 1.0 kN/s until failure occurred. The interfacial shear strength was calculated from the peak load using the following expression:

$$\tau = \frac{P}{A} \tag{2}$$

where τ is the nominal shear strength (MPa), P is the peak load (N), and A is the total effective bonded area (mm^2). For the principal double-face analysis, A = 60000 mm^2.

The specimen was monitored for interface cracking, sliding, substrate cracking, and other failure features. All push-out records, including PUN-Z-1, were retained in the descriptive dataset. No test record was excluded on the basis of visual observation or an unquantified fixture concern. Any future exclusion would require recorded, objective evidence such as measured load eccentricity, verified support spacing, an LVDT-difference threshold, a bending-strain threshold, or a documented fracture plane that departs from the interface.

3. Experimental Results and Discussion

3.1 Interfacial Splitting Tensile Test Results

3.1.1 Failure Modes

During splitting-tensile loading, the available observations were interpreted in three stages: an approximately linear pre-cracking stage, crack initiation and propagation near the interface, and final separation. Because no strain field or acoustic-emission measurement was performed, this description is limited to visible cracking and the recorded load response.

Among the three SPN-Z specimens, SPN-Z-1 and SPN-Z-2 showed Type A interfacial failure and SPN-Z-3 showed Type B mixed failure. Among the three SPU-G specimens, all three showed Type C predominantly interfacial failure. The rougher fracture appearance of the SPN-Z specimens is an observed macroscopic feature; it does not by itself establish a microstructural mechanism. The untreated UHPC–grout specimens (SPU-G) exhibited comparatively smooth fracture surfaces with

limited visible grout residue. This observation is consistent with lower visible mechanical interlocking at the untreated surface, but no direct microstructural characterization was conducted.

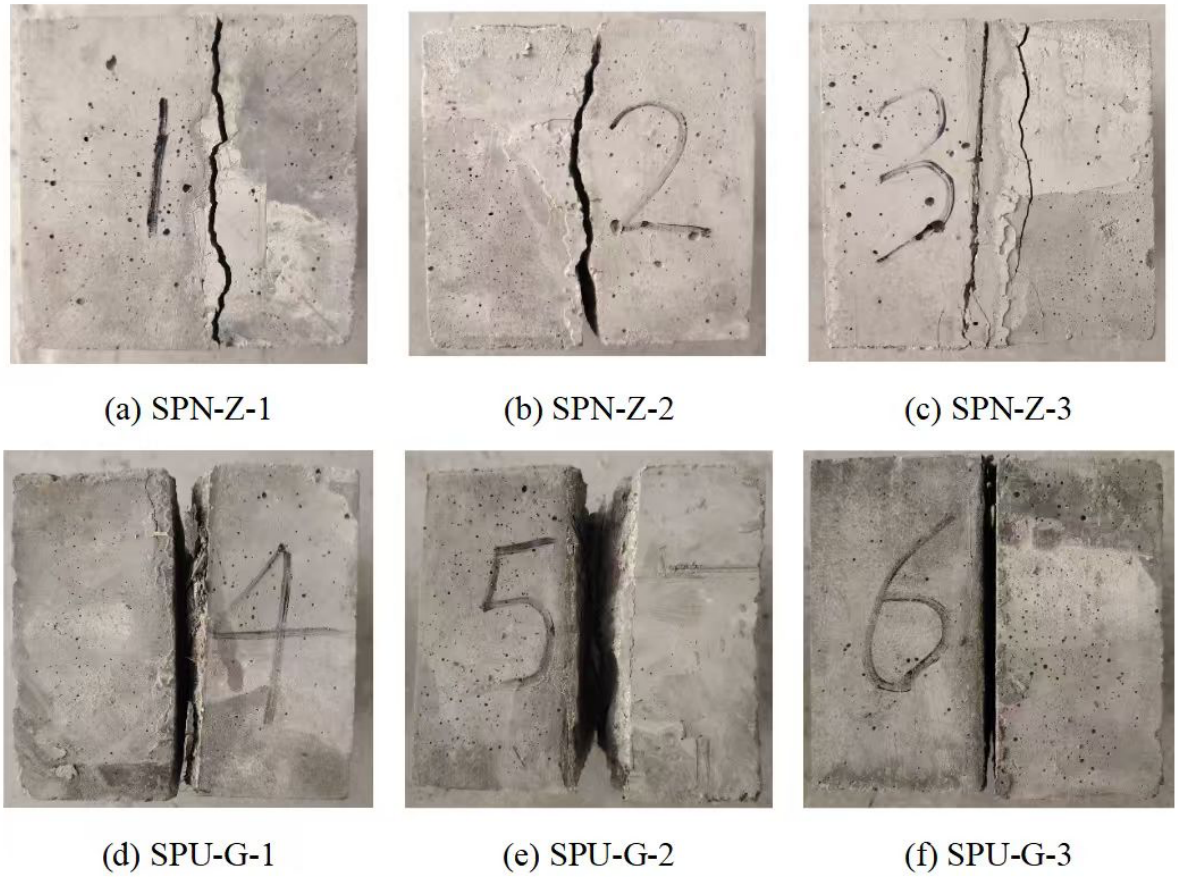


Fig. 3. Fracture patterns of bonded-interface splitting-tensile specimens: (a–c) SPN-Z-1 to SPN-Z-3; (d–f) SPU-G-1 to SPU-G-3

3.1.2 Splitting Tensile Strength

The splitting-tensile strength was calculated using the expression in Section 2.4.1. The reported specimen values yielded 3.45 ± 0.02 MPa for SPN-Z and 3.54 ± 0.12 MPa for SPU-G (mean ± sample SD, n = 3 per group). The two-sided Welch test gave p = 0.324. This small, confounded dataset does not establish equivalence or identify an independent effect of surface treatment. For each group, the 95% CI of the mean was calculated as mean ± t0.975, n−1 × SD/√n. The CIs are reported in Tables 5, 6, and 8. They describe the uncertainty of the observed group means; they do not resolve the confounding of substrate type and surface treatment.

For comparison with monolithic material, the normalized interface index is defined by the following LaTeX expression:

$$n = \frac{f_{ts}}{f_c} \tag{3}$$

where f_{ts} is the interface splitting tensile strength and f_c is the monolithic splitting tensile strength of the corresponding substrate material. Based on the numerical entries currently shown in Table 5, $f_c = 4.04$ MPa for NC and $f_c = 5.40$ MPa for UHPC; the latter replaces the internally inconsistent value of 5.73 MPa and must be verified against the original test sheet. The monolithic NC value of 4.04 MPa was calculated from the three entries in Table 5. The three UHPC entries give a confirmed mean of 5.40 MPa. The normalized indices calculated from these reported values are approximately 0.85 for SPN-Z and 0.66 for SPU-G.

Table 5. Splitting tensile strength of monolithic specimens

Specimen ID	Peak load (kN)	Splitting tensile	Group mean	95% CI of group
NC-1	160.40	4.54	4.04	2.79–5.28
NC-2	125.38	3.54	4.04	2.79–5.28
NC-3	142.19	4.02	4.04	2.79–5.28
UHPC-1	167.76	4.75	5.40	4.00–6.81
UHPC-2	201.89	5.71	5.40	4.00–6.81
UHPC-3	203.35	5.75	5.40	4.00–6.81

Table 6. Splitting tensile strength of bonded interfaces

Specimen ID	Interface	Peak load (kN)	f_ts (MPa)	Mean ± SD (MPa)	95% CI (MPa)	CV (%)	Failure mode
SPN-Z-1	NC–grout, chiseled	121.89	3.45	3.45 ± 0.02	3.40–3.50	0.58	A
SPN-Z-2	NC–grout, chiseled	122.58	3.47	3.45 ± 0.02	3.40–3.50	0.58	A
SPN-Z-3	NC–grout, chiseled	121.20	3.43	3.45 ± 0.02	3.40–3.50	0.58	B
SPU-G-1	UHPC–grout, untreated	124.28	3.52	3.54 ± 0.12	3.25–3.82	3.28	C
SPU-G-2	UHPC–grout, untreated	129.22	3.66	3.54 ± 0.12	3.25–3.82	3.28	C
SPU-G-3	UHPC–grout, untreated	121.26	3.43	3.54 ± 0.12	3.25–3.82	3.28	C

3.2 Push-Out Test Results

3.2.1 Failure Modes

The push-out failure modes are reported by specimen code. PUN-Z-1, PUN-Z-2, and PUN-Z-3 are retained as valid double-face records and are all included in the PUN-Z descriptive dataset. PUN-Z-2 and PUN-Z-3 showed mixed or interface-related failure features, whereas the untreated UHPC-grout specimens predominantly showed Type C interfacial shear failure. The original file noted a fixture concern for PUN-Z-1, but no quantitative eccentricity, support-spacing, LVDT, bending-strain, or fracture-plane criterion was available to justify exclusion. PUN-Z-1 is therefore included in the PUN-Z mean. The available evidence is insufficient to attribute failure-mode differences solely to chiselling because substrate type and surface treatment were changed together.

The untreated UHPC–grout specimens showed relatively flat failure surfaces in the available records. This macroscopic observation is described without inferring a chemical or microstructural bonding mechanism.

3.2.2 Load–Displacement Curve Analysis

Relative slip was calculated from the displacement-transducer readings and paired with the measured load. Figure 5 displays the available raw curves for PUN-Z-1, PUN-Z-2, PUN-Z-3, PUU-G-2-1, and PUU-G-2-2. PUN-Z-1 is included in the primary PUN-Z descriptive dataset. The original fixture concern is not used as an exclusion rationale because no quantitative diagnostic records or repeat-test data were available.

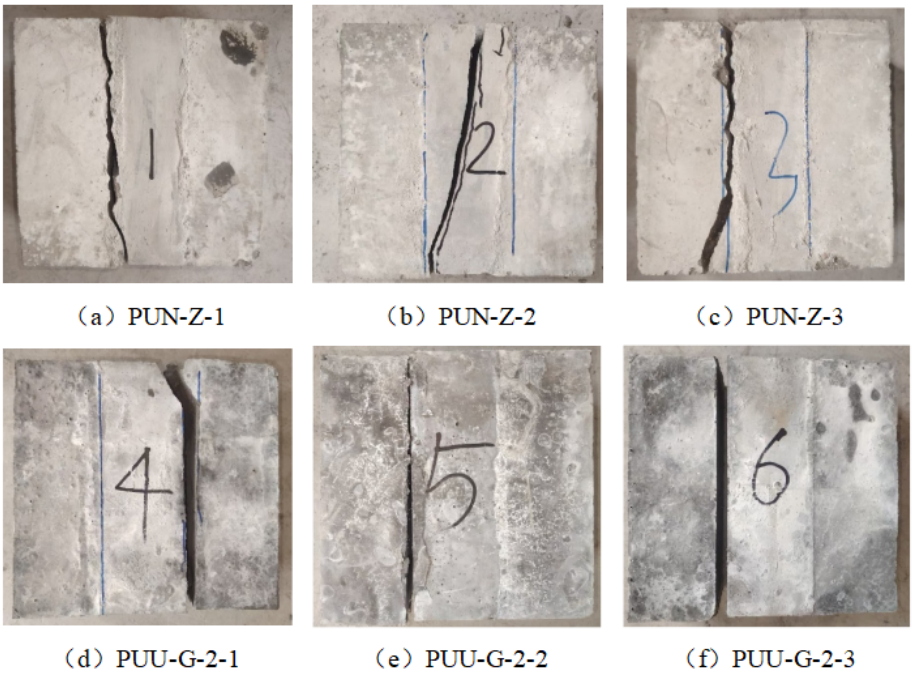


Fig. 4. Failure modes of push-out specimens: (a–c) PUN-Z-1 to PUN-Z-3; (d–e) PUU-G-2-1 and PUU-G-2-2. PUU-G-2-3 was a strength-check specimen and is not included in the primary double-face PUU-G dataset. PUN-Z-1 is included in the primary PUN-Z descriptive dataset

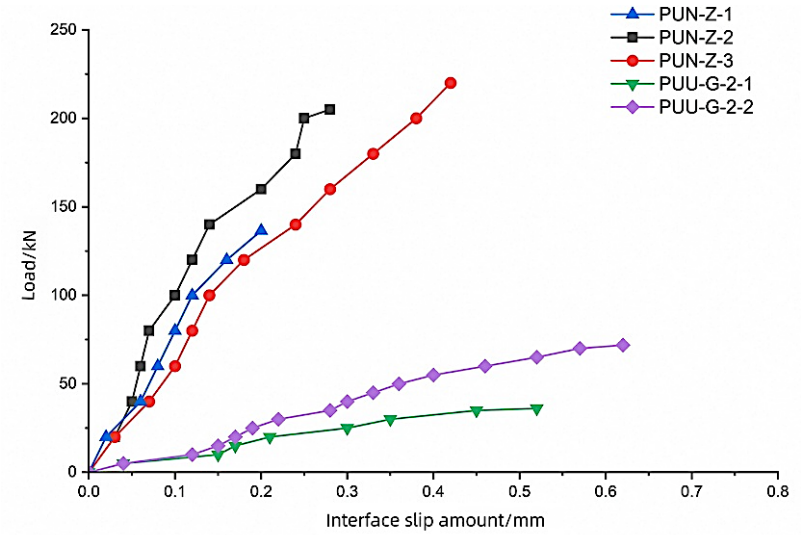


Fig. 5. Interfacial load–slip curves

The available load–slip curves show higher recorded peak loads for the PUN-Z observations than for the two double-face PUU-G observations. The corresponding nominal shear strengths were 2.92, 3.42, and 3.66 MPa for PUN-Z-1 to PUN-Z-3 and 1.03 and 1.20 MPa for PUU-G-2-1 and PUU-G-2-2. This is a descriptive, exploratory comparison only. In particular, the PUU-G group has n = 2, which is insufficient to support general inference, and the two groups simultaneously differ in substrate type and surface treatment. Any statement of improved "ductility" would require a pre-defined displacement- or energy-based metric and is not inferred from the plotted curve shape.

3.2.3 Interfacial Shear Stiffness

The apparent interfacial shear stiffness k was defined as the slope obtained by linear regression over the 10%–40% peak-load interval of each available load–slip curve. Because the manuscript contains no independent machine-compliance calibration, these values are designated as apparent stiffness. The available specimen-level slope labels are reported in Table 9, including the raw PUN-Z-1 value of 833 kN/mm:

$$k = \frac{\Delta P}{\Delta s} \ (0.10P_{max} \le P \le 0.40P_{max}) \quad (4)$$

Here P is load, and s is relative slip. The 10%–40% Pmax window is stated to define the reported apparent-stiffness slope. Because the original numerical load–slip pairs are unavailable, no individual regression equation, R^2 value, or fit-acceptance threshold is asserted in this revision. The existing slope labels for all five raw records are reported transparently in Table 9.

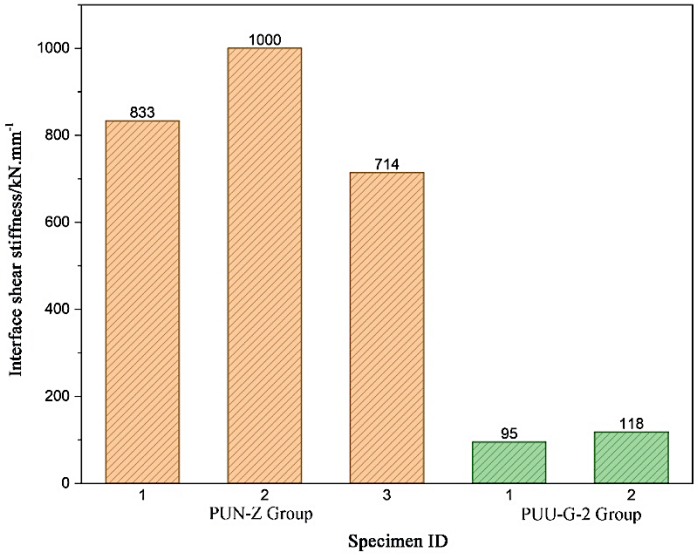


Fig. 6. Available apparent interfacial shear-stiffness labels

3.2.4 Shear Strength

Table 7 reports all available double-face push-out records with geometry identified explicitly. PUN-Z-1 is included in the primary PUN-Z descriptive dataset because no objective quantitative exclusion evidence is available. The three PUN-Z records give 3.33 ± 0.38 MPa (n = 3; 95% CI: 2.40–4.27 MPa). The two PUU-G records give 1.12 ± 0.12 MPa (n = 2; 95% CI: 0.03–2.20 MPa). The corresponding absolute mean difference is 2.22 MPa, and the strength ratio is 2.99. No inferential test is used for the push-out comparison: the PUU-G group has n = 2, and the comparison is exploratory only.

Table 7. Interface push-out test shear strengths

Specimen ID	Bonded area (mm^2)	Failure load, P (kN)	Shear strength, τ (MPa)	Record status	Failure mode
PUN-Z-1	60000	175.20	2.92	Included in PUN-Z primary dataset (n = 3)	Interfacial shear with fixture-related observation
PUN-Z-2	60000	205.00	3.42	Included in PUN-Z primary dataset (n = 3)	B
PUN-Z-3	60000	219.48	3.66	Included in PUN-Z primary dataset (n = 3)	A
PUU-G-2-1	60000	61.80	1.03	Included in PUU-G summary (n = 2)	C
PUU-G-2-2	60000	71.85	1.20	Included in PUU-G summary (n = 2)	C

Note: PUN-Z-1 is retained as a raw record. The original record noted a fixture concern, but the available files contain no quantitative eccentricity, actual support-spacing, LVDT-difference, bending-strain, or fracture-plane data that could support an objective exclusion decision. PUU-G-2-1 and PUU-G-2-2 are the only double-face UHPC–grout records. Single-face records are not included in any double-face summary. The group summaries and 95% CIs are reported in Table 8.

Table 8. Descriptive double-face push-out group summaries and 95% confidence intervals

Dataset/purpose	Records	n	Mean ± SD (MPa)	95% CI (MPa)	Interpretation
PUN-Z primary descriptive dataset	PUN-Z-1/2/3	3	3.33 ± 0.38	2.40–4.27	Descriptive raw summary; PUN-Z-1 retained because no objective quantitative exclusion evidence is available
PUU-G double-face dataset	PUU-G-2-1/2	2	1.12 ± 0.12	0.03–2.20	Exploratory only; n = 2

Note: UN-Z-1 is included in the primary PUN-Z descriptive dataset because no objective quantitative exclusion criterion is available. The PUU-G double-face dataset comprises PUU-G-2-1 and PUU-G-2-2 only and is exploratory because n = 2.

Table 9. Specimen-level apparent interfacial shear stiffness and available regression information

Specimen ID	10%–40% Pmax interval (kN)	Apparent stiffness (kN/mm)	Record status
PUN-Z-1	17.52–70.08	833	Raw record retained
PUN-Z-2	20.50–82.00	1000	Raw record retained
PUN-Z-3	21.95–87.79	714	Raw record retained
PUU-G-2-1	6.18–24.72	95	Raw record retained
PUU-G-2-2	7.19–28.74	118	Raw record retained

3.3 Discussion

Because the present design does not distinguish chiselling from changing the substrate material, the observed group difference cannot be interpreted as an independent causal effect of either factor. For the double-face datasets, PUN-Z gave 3.33 ± 0.38 MPa (n = 3; 95% CI: 2.40–4.27 MPa) and PUU-G gave 1.12 ± 0.12 MPa (n = 2; 95% CI: 0.03–2.20 MPa). The observed absolute difference is 2.22 MPa and the strength ratio is 2.99. These are exploratory observed values, not a generalizable treatment effect. PUN-Z-1 is included in the PUN-Z primary dataset because no objective quantitative exclusion criterion is available. The wide 95% CIs, especially for the two-specimen PUU-G group, show the statistical uncertainty associated with the limited replication. Push-out results are therefore reported as descriptive observations without a significance claim. At least three geometry-consistent specimens are required in each group before attempting a replicated comparison; a factorial design must also hold either substrate type or surface treatment constant to estimate the effect of the other factor.

The splitting-tensile means were 3.45 ± 0.02 MPa for SPN-Z (95% CI: 3.40–3.50 MPa) and 3.54 ± 0.12 MPa for SPU-G (95% CI: 3.25–3.82 MPa), with n = 3 in each group. The observed absolute difference was 0.09 MPa and the strength ratio was 1.03. The reported two-sided Welch test gave p = 0.324. This small, confounded dataset does not demonstrate equality of the two interfaces or identify an independent surface-treatment effect. The observed failure appearances of the chiseled NC–grout and untreated UHPC–grout records may reflect differences in contact-area complexity and mechanical interlocking. Contributions from hydration-product deposition or chemical adhesion were not measured. No mechanism is claimed as established; SEM/EDS, three-dimensional roughness characterization, and controlled curing measurements would be required to test these hypotheses.

This study has five principal limitations. First, substrate type and surface treatment were not separated experimentally. Second, the double-face PUU-G group contains only two specimens, which is insufficient to support general or inferential conclusions; additional testing to at least three geometry-consistent specimens per group is required. Third, PUN-Z-1 could not be objectively evaluated for exclusion because the required quantitative diagnostic records and repeat

tests were unavailable; it is therefore included in the primary PUN-Z descriptive dataset. Fourth, no microstructural characterization or quantitative roughness measurement was performed. Fifth, the tests were short-term static laboratory tests and did not address seawater exposure, durability, fatigue, or cyclic loading. All interpretations and applications are limited accordingly.

4. Conclusions

Within the present short-term static laboratory program, the following conclusions are limited to the available records and conditions:

- The present programmed examined two distinct interfaces—UHPC–grout and NC–grout—rather than a direct UHPC–NC interface. Because untreated UHPC–grout specimens were compared with *chiseled* NC–grout specimens, the independent effects of substrate type and *chiseling* cannot be separated.
- The push-out records are exploratory rather than inferential. The PUN-Z dataset, including PUN-Z-1, gave 3.33 ± 0.38 MPa (n = 3; 95% CI: 2.40–4.27 MPa), whereas the two double-face PUU-G records gave 1.12 ± 0.12 MPa (n = 2; 95% CI: 0.03–2.20 MPa). The absolute difference was 2.22 MPa and the strength ratio was 2.99. These values cannot be attributed independently to chiselling or to substrate material, and n = 2 is insufficient for a general conclusion.
- The splitting-tensile strengths were 3.45 ± 0.02 MPa for SPN-Z (95% CI: 3.40–3.50 MPa) and 3.54 ± 0.12 MPa for SPU-G (95% CI: 3.25–3.82 MPa). The observed absolute difference was 0.09 MPa and the strength ratio was 1.03. The reported two-sided Welch test gave p = 0.324; this result does not establish equivalence or an independent surface-treatment effect.
- The observed change from predominantly interfacial failure in untreated UHPC–grout records to more mixed failure appearances in the NC–grout records is a macroscopic observation. Its cause requires a factorial treatment design, quantitative roughness measurements, original load–slip data with regression outputs, an objective repeat test or exclusion assessment for PUN-Z-1, and at least three replicated double-face specimens per group. No conclusion regarding long-term marine performance, durability, or cyclic loading is drawn from this study.

For engineering application, surface preparation is a construction variable requiring controlled specification and quality assurance; however, no design recommendation beyond the present laboratory conditions is made. Future experiments should include untreated NC and chiseled UHPC control groups, identical double-face geometries, at least three specimens per group, quantitative roughness data, objectively recorded fixture diagnostics, and durability/cyclic-loading exposure.

Foundation Project

Liuzhou City Vocational College Scientific Research Project: Application Research on Ultra-High Impermeability Grouting Material Reinforcing Underwater Aged Concrete Structures Empowered by AI (2026KYZD01)

References

[1] Ding J, Zhu J, Kang J. Bonding properties and mechanism of the interface between precast UHPC and post-cast UHPC. Structures. 2022;43:822-833. https://doi.org/10.1016/j.istruc.2022.07.016
[2] Zhang Y, Zhu P, Liao Z, Wang L. Interfacial bond properties between normal strength concrete substrate and ultra-high performance concrete as a repair material. Construction and Building Materials. 2020;235:117431. https://doi.org/10.1016/j.conbuildmat.2019.117431
[3] Zhang Y, Zhu P, Wang X, Wu J. Shear properties of the interface between ultra-high performance concrete and normal strength concrete. Construction and Building Materials. 2020;248:118455. https://doi.org/10.1016/j.conbuildmat.2020.118455
[4] Tayeh BA, Abu Bakar BH, Megat Johari MA. Characterization of the interfacial bond between old concrete substrate and ultra high performance fiber concrete repair composite. Materials and Structures. 2012;46(5):743-753. https://doi.org/10.1617/s11527-012-9931-1
[5] Tayeh BA, Abu Bakar BH, Megat Johari MA, Voo YL. Evaluation of bond strength between normal concrete substrate and ultra high performance fiber concrete as a repair material. Procedia Engineering. 2013;54:554-563. https://doi.org/10.1016/j.proeng.2013.03.050

[6] Valikhani A, Jahromi AJ, Mantawy IM, Azizinamini A. Experimental evaluation of concrete-to-UHPC bond strength with correlation to surface roughness for repair application. Construction and Building Materials. 2020;238:117753. https://doi.org/10.1016/j.conbuildmat.2019.117753
[7] Zhang B, Yu J, Chen W, Liu H, Li H, Guo H. Experimental study on bond performance of NC-UHPC interfaces with different roughness and substrate strength. Materials. 2023;16(7):2708. https://doi.org/10.3390/ma16072708
[8] Graybeal BA. Material Property Characterization of Ultra-High Performance Concrete. Report No.: FHWA-HRT-06-103. Federal Highway Administration; 2006.
[9] Du C, Liu X, Liu Y, Tong T. Prediction of the interface shear strength between ultra-high-performance concrete and normal concrete using artificial neural networks. Materials. 2021;14(19):5707. https://doi.org/10.3390/ma14195707
[10] Zhang B, Yu J, Chen W, Chen J, Li H, Niu J. Interface shear failure behavior between normal concrete (NC) and ultra-high performance concrete (UHPC). International Journal of Concrete Structures and Materials. 2024;18:18. https://doi.org/10.1186/s40069-023-00657-6
[11] Zhao YC, Lei HG, Guo LK, Lu GY. Experimental investigation on interface performance of UHPC-strengthened NC structure through push-out tests. Materials. 2023;16(5):1766. https://doi.org/10.3390/ma16051766
[12] Feng S, Xiao H, Liu M, Zhang F, Lu M. Shear behaviour of interface between normal-strength concrete and UHPC: Experiment and predictive model. Construction and Building Materials. 2022;342:127919. https://doi.org/10.1016/j.conbuildmat.2022.127919
[13] Harris DK, Carbonell Muñoz MA, Gheitasi A, Ahlborn TM, Rush SV. The challenges related to interface bond characterization of ultra-high-performance concrete with implications for bridge rehabilitation practices. Advances in Civil Engineering Materials. 2015;4(2):75-101. https://doi.org/10.1520/ACEM20140034
[14] Jang HO, Lee HS, Cho K, Kim J. Experimental study on shear performance of plain construction joints integrated with ultra-high performance concrete (UHPC). Construction and Building Materials. 2017;152:16-23. https://doi.org/10.1016/j.conbuildmat.2017.06.156
[15] Xu L, Yao Y, Li Y, Su J, Wu Y. Review of the interfacial bonding properties between ultrahigh-performance concrete and normal concrete. Applied Sciences. 2023;13(11):6697. https://doi.org/10.3390/app13116697